**Cell Reports, Volume *34***

## Supplemental Information

# Systematic analysis of purified astrocytes after SCI unveils *Zeb2os* function during astrogliosis

**Haichao Wei, Xizi Wu, Yanan You, Raquel Cuevas-Diaz Duran, Yiyan Zheng, K. Lakshmi Narayanan, Bo Hai, Xu Li, Neha Tallapragada, Tanuj J. Prajapati, Dong H. Kim, Benjamin Deneen, Qi-Lin Cao, and Jia Qian Wu**

**Cell Reports, Volume *34***

## Supplemental Information

# Systematic analysis of purified astrocytes after SCI unveils *Zeb2os* function during astrogliosis

**Haichao Wei, Xizi Wu, Yanan You, Raquel Cuevas-Diaz Duran, Yiyan Zheng, K. Lakshmi Narayanan, Bo Hai, Xu Li, Neha Tallapragada, Tanuj J. Prajapati, Dong H. Kim, Benjamin Deneen, Qi-Lin Cao, and Jia Qian Wu**

A

| Category | Timepoint | Upregulated in SCI | Downregulated in SCI | Total DEGs |
|---|---|---|---|---|
| Protein-coding genes | 2D | 2275 | 810 | 3085 |
| | 7D | 2811 | 1802 | 4613 |
| | 1M | 1751 | 381 | 2132 |
| | 3M | 1347 | 34 | 1381 |
| lncRNAs | 2D | 130 | 233 | 363 |
| | 7D | 212 | 401 | 613 |
| | 1M | 125 | 88 | 213 |
| | 3M | 64 | 16 | 80 |
| Transcription factors | 2D | 151 | 66 | 217 |
| | 7D | 183 | 110 | 293 |
| | 1M | 104 | 27 | 131 |
| | 3M | 80 | 2 | 82 |

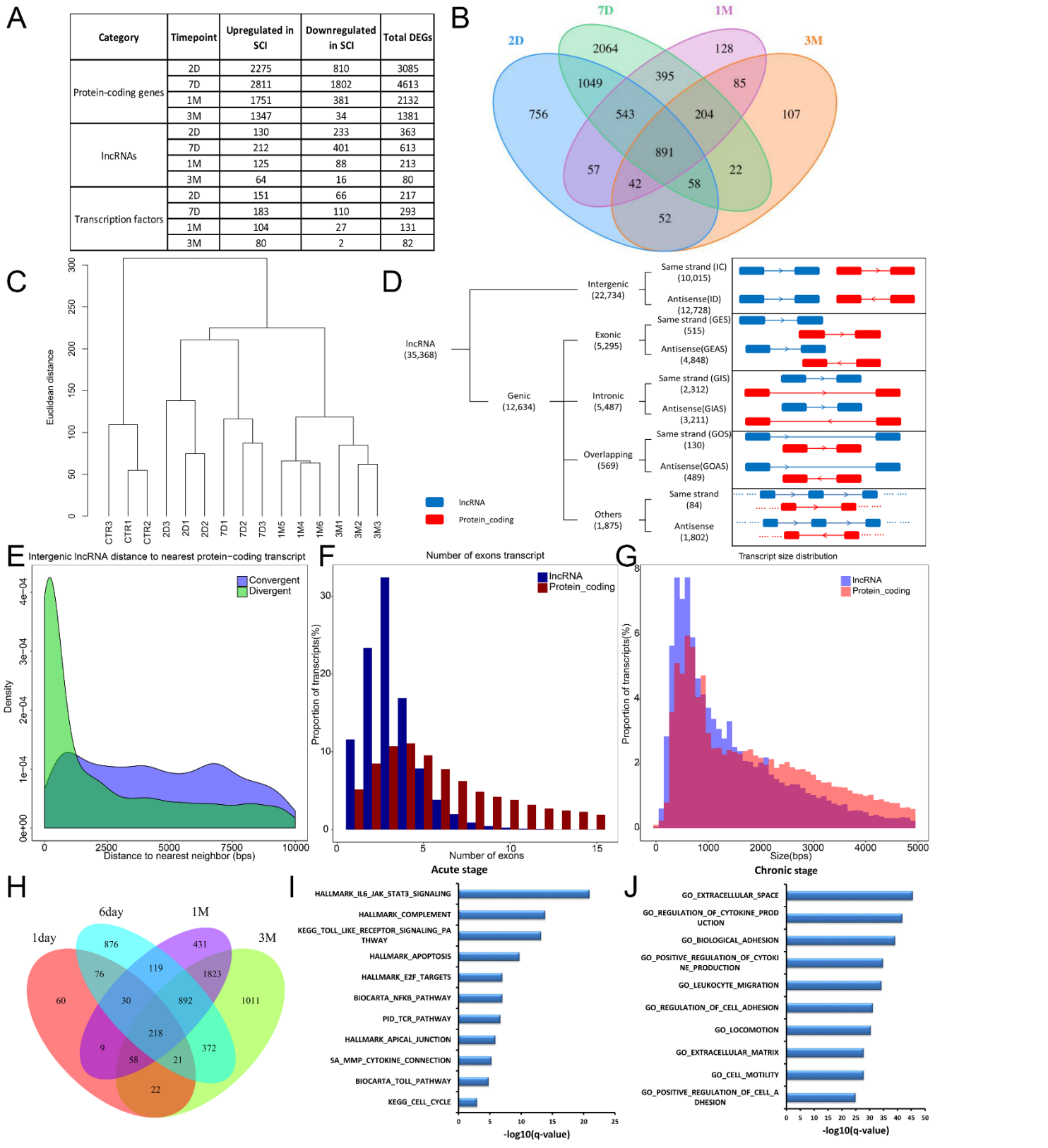


**Figure S1** Related to Figure 1. **(A)** Differentially expressed protein-coding genes, lncRNAs, and transcription factors at 2D (2 days), 7D (7 days), 1M (1 month), and 3M (3 months). Cutoff: log2|fold-change| > 1, FDR < 0.05, at least one samples' FPKM > 1. **(B)** Venn diagram depicting the DEGs whose expression overlaps at different injury stages. **(C)** A consensus dendrogram was constructed from the Euclidean distance of log2-transformed FPKM values**. (D)** Categorization of lncRNAs in the mouse genome. Annotated mouse lncRNAs were classified based on their genomic locations relative to protein-coding genes (see Methods section for details). The number of lncRNAs in each class and subclass is indicated in parenthesis. Based on the combined lncRNA annotations,

64.3% (22,734 of 35,368) of sequences encoding lncRNA transcripts were located in intergenic regions. **(E)** Distribution of the distance from IC (same strand) lncRNAs (blue) or ID (antisense) lncRNAs (green) to the closest protein-coding gene. The distances from divergent lncRNAs (on the opposite strand from the closest protein-coding gene to the closest protein-coding gene are shorter than those of convergent lncRNAs (on the same strand as the closest protein-coding gene). **(F)** The number of exons per transcript for lncRNA (blue) and protein-coding genes (red). The median number of exons in mouse lncRNA transcripts is 3. **(G)** Distribution of the transcript sizes of lncRNAs (blue) and protein-coding genes (red). The median size of lncRNA transcripts was approximately 1,169 bp, and the median transcript size of protein-coding genes was 1,828 bp. **(H)** Venn diagram depicting DEGs whose expression overlaps at different SCI time points in rat. **(I, J)** Top enriched gene-sets for the common DEGs at acute **(I)** and chronic **(J)** SCI stages between mouse and rat.

A

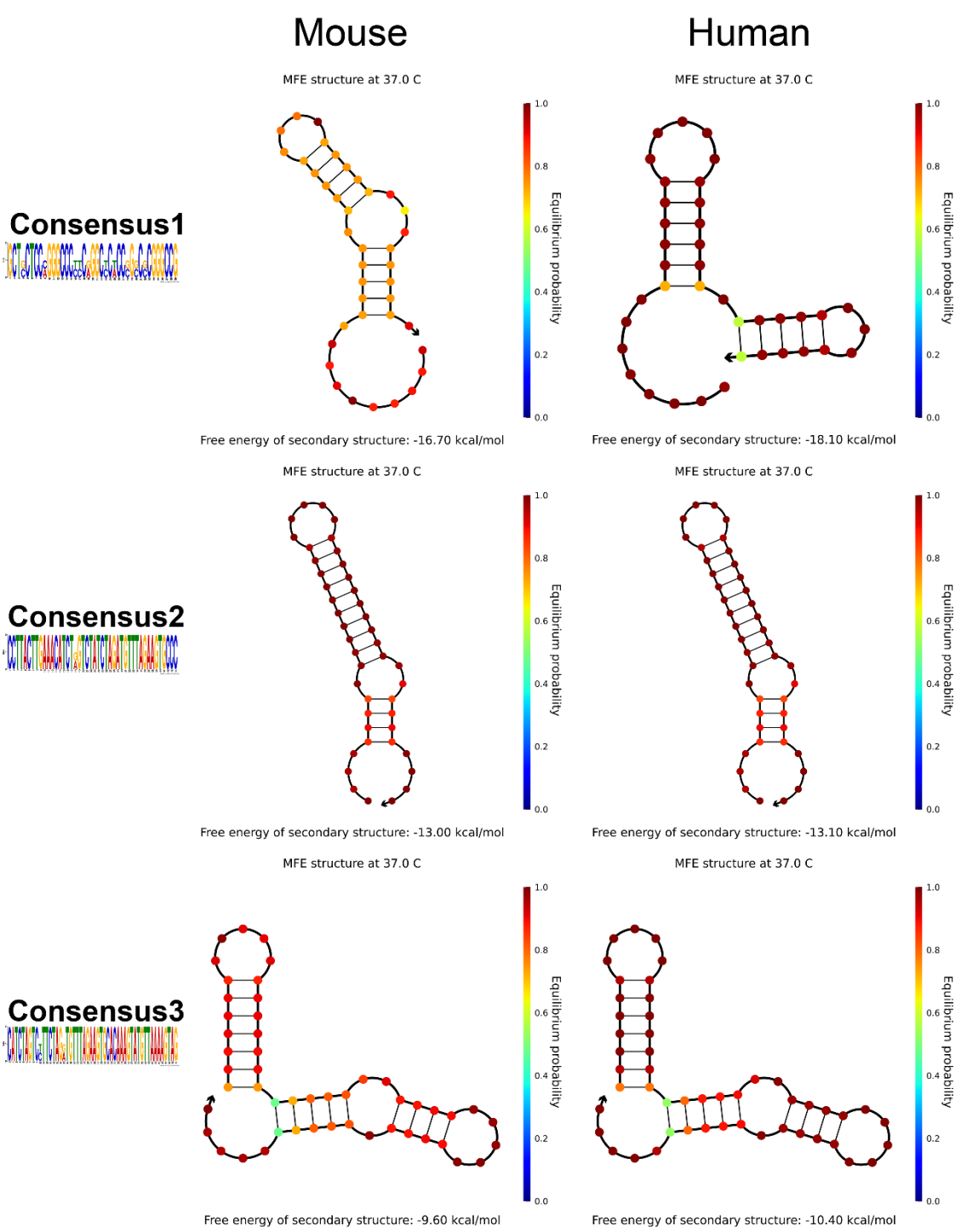
Mouse
Human
Consensus1
Consensus2
Consensus3
MFE structure at 37.0 C
Equilibrium probability
Free energy of secondary structure: -16.70 kcal/mol
Free energy of secondary structure: -18.10 kcal/mol
Free energy of secondary structure: -13.00 kcal/mol
Free energy of secondary structure: -13.10 kcal/mol
Free energy of secondary structure: -9.60 kcal/mol
Free energy of secondary structure: -10.40 kcal/mol

B

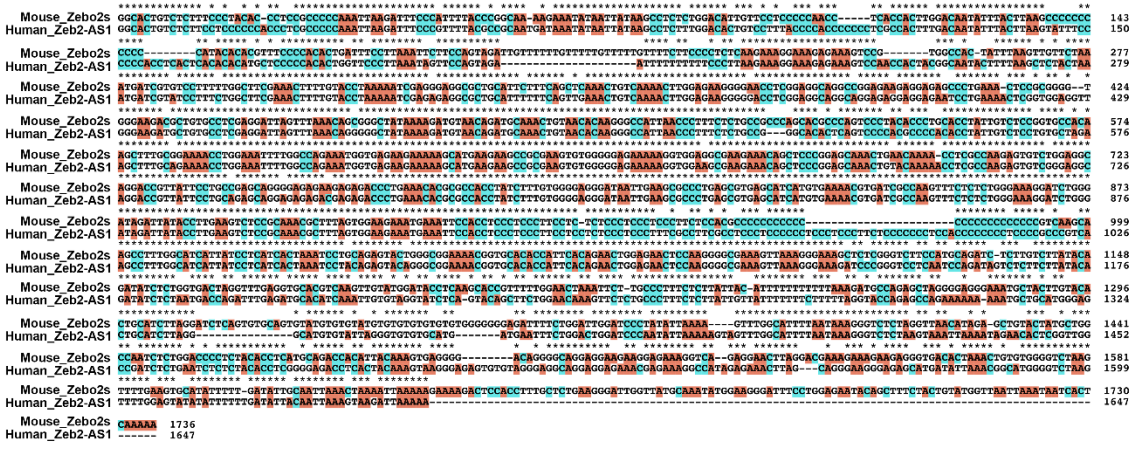
Mouse_Zebo2s
Human_Zeb2-AS1

**Figure S2** Related to Figure 1 and 2. **(A)** The consensus regions of *2900097C17Rik* exhibit similar secondary structures between human and mouse. **(B)** *Zeb2os* is highly conserved between human (Human_*ZEB2-AS1*, ENST00000427278.8) and mouse (Mouse_*Zeb2os*, ENSMUST00000127150.8).

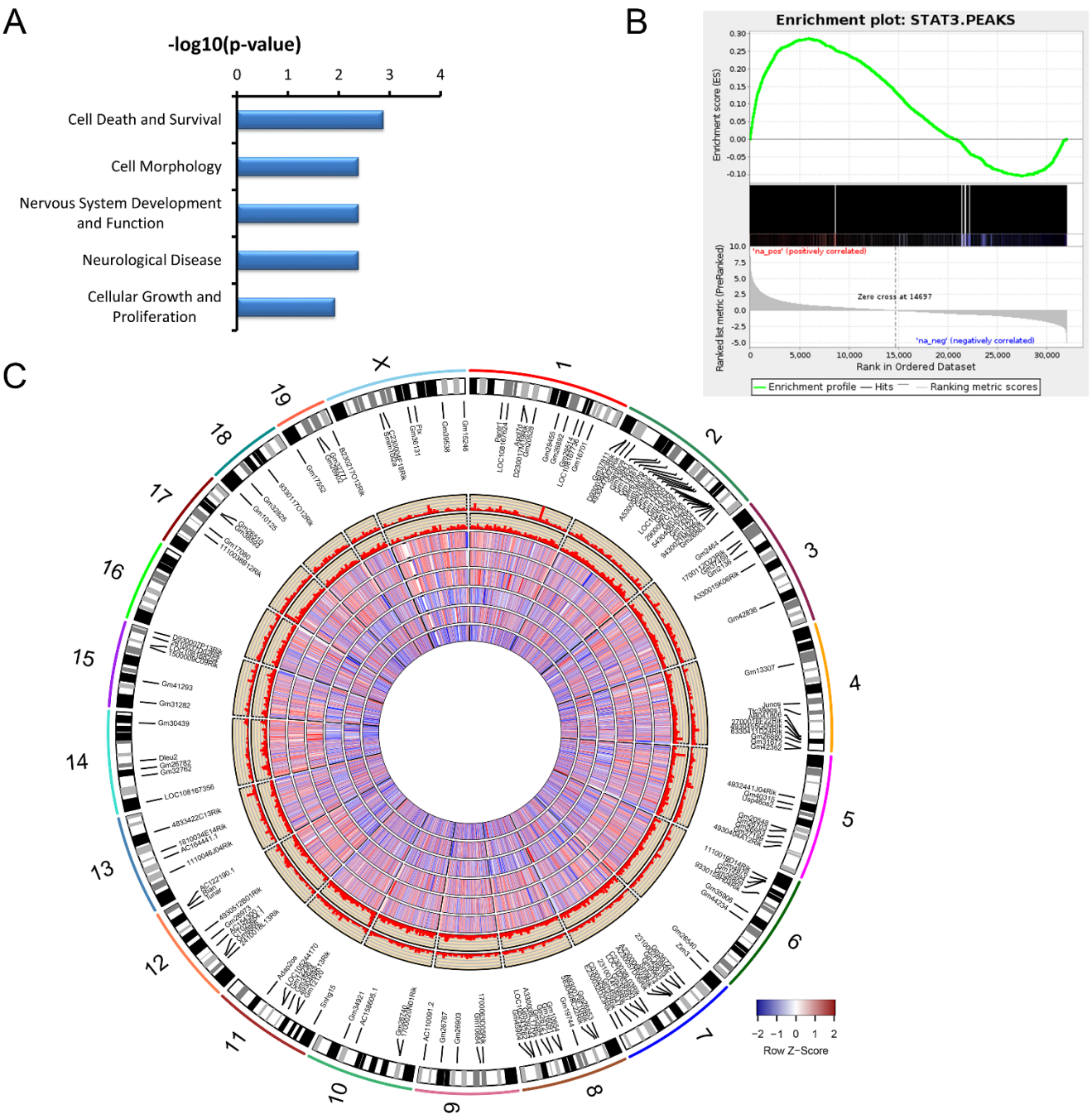


**Figure S3 ChIP-Seq analysis of STAT3 in Sham and SCI epicenter tissue**. Related to Figure 1. **(A)** Highly enriched gene sets of STAT3 binding sites in SCI samples. **(B)** Correlation of STAT3 binding targets with the DEGs identified using Gene Set Enrichment Analysis. Genes ranked by fold-change comparing 7 days post injury with control samples. Statistically Normalized Enrichment Score (NES = 1.33) of STAT3 binding peaks after injury (nominal *p*-value = 0, FDR = 0). **(C)** Circos plot representing STAT3 binding peaks and gene expression levels. Tracks 1 shows DE lncRNAs with STAT3-bound peaks in their promoter after SCI; Tracks 2-3 display the ChIP-Seq binding peaks at 7D post SCI and Sham samples. Tracks 4-9 depict log2-transformed FPKM values of genes expressed in CTR1, CTR2, CTR3, 7D1, 7D2, and 7D3 samples as a heatmap. Labels indicate differentially expressed lncRNAs (FDR < 0.05, fold-change > 2 and FPKM > 1 in at least one sample) which are the binding targets of STAT3 in SCI samples at 7D post SCI.

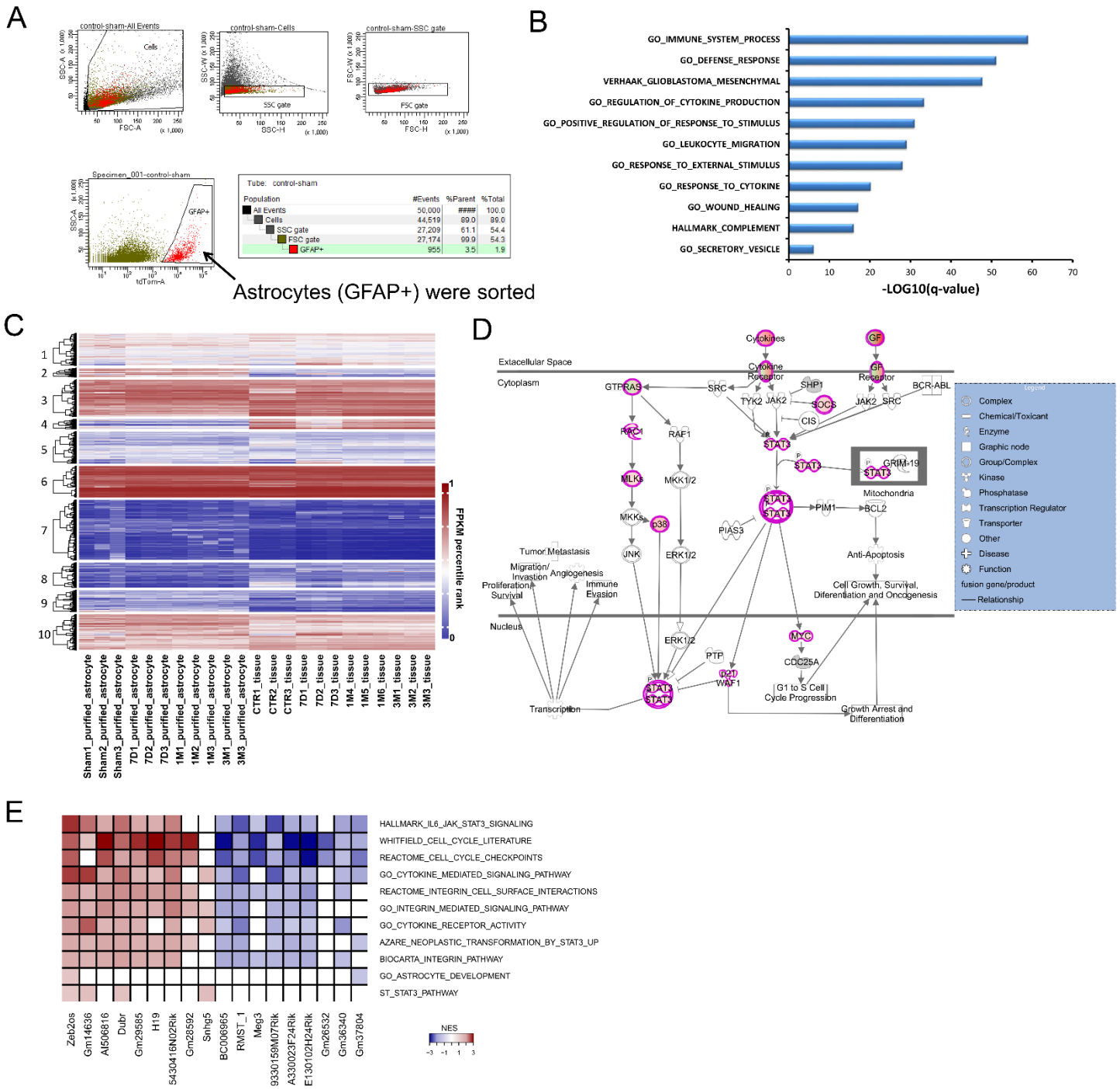


**Figure S4** Related to Figure 2. **(A)** Representative FACS workflow and gating strategy for purifying tdTomato positive astrocytes from spinal cord tissue segments (5 mm) at the SCI epicenter encompassing the glial scar. **(B)** Enriched gene sets for DEGs in common among all stages after SCI in purified astrocytes. **(C)** Hierarchical clustering of genes expressed in purified astrocytes and spinal cord tissue samples after SCI. **(D)** Enrichment of the STAT3 pathway (FDR < 0.05) in purified astrocytes at 7D after SCI. Intensity of the red (increased expression) and green (decreased expression) color indicates the degree of change (log2|fold-change|) in genes expression**. (E)** Heatmap representing an association matrix of conserved lncRNAs and enriched functional terms.

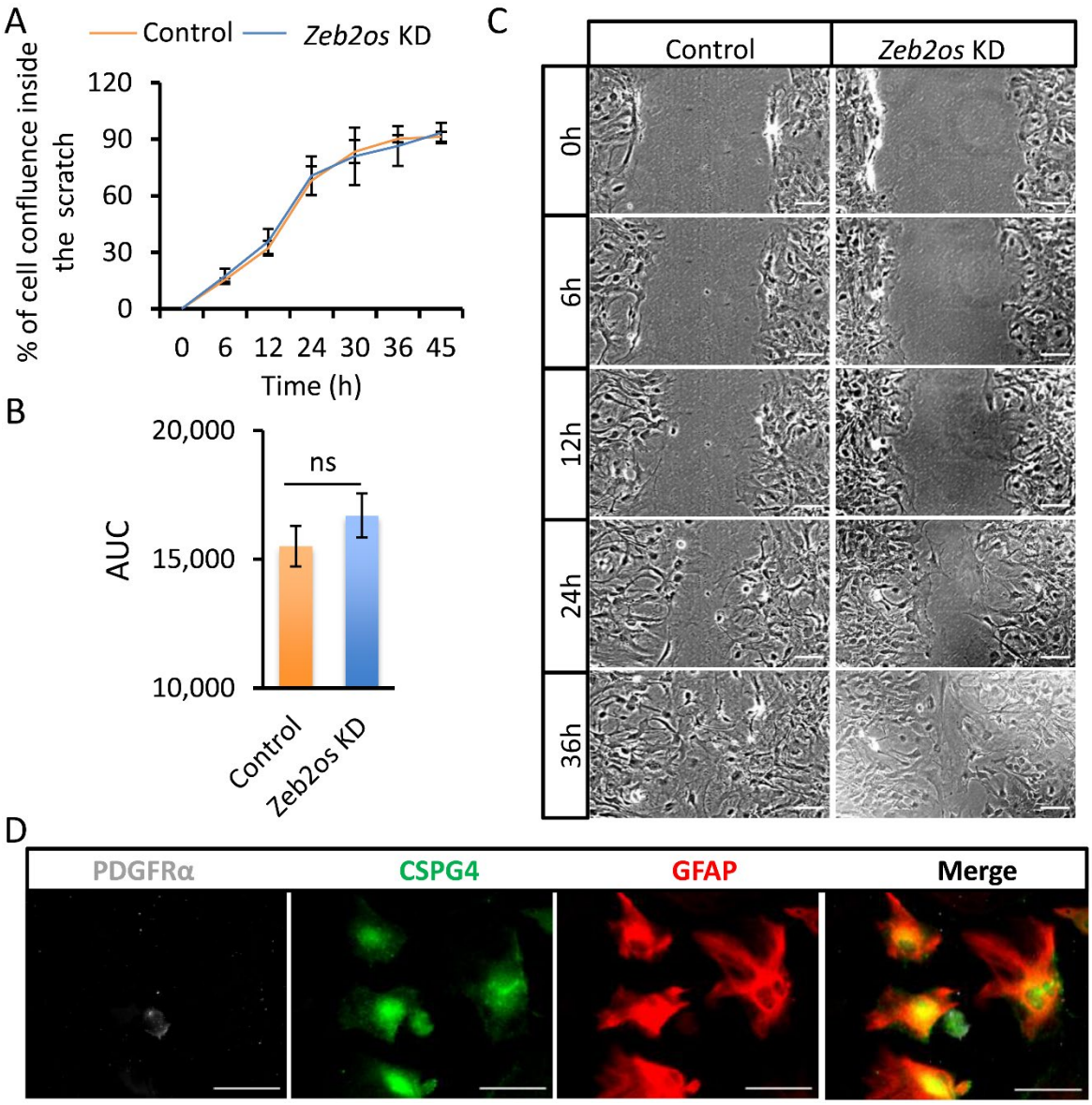


**Figure S5** Related to Figure 4. **(A)** The temporal profile of the *Zeb2os* knockdown and control astrocyte confluences inside the scratch. The trend line shows the average value of temporal profile and presented as mean ± SD ($n$ = 4). **(B)** The AUC is calculated and presented as mean ± SD. An independent $t$-test was performed to compared the difference between groups; ns, no significant difference between groups. **(C)** Brightfield images show astrocytes migration to the scratch wound at various time points after the scratch (Scale bar = 100 μm). **(D)** CSPG4 expression in images show individual channels and various combinations of immunofluorescence staining for PDGFRα (white), CSPG4 (green) and GFAP (red). CSPG4 is expressed in GFAP labeled astrocytes as well as PDGFRα labeled cells (Scale bar = 40 μm).

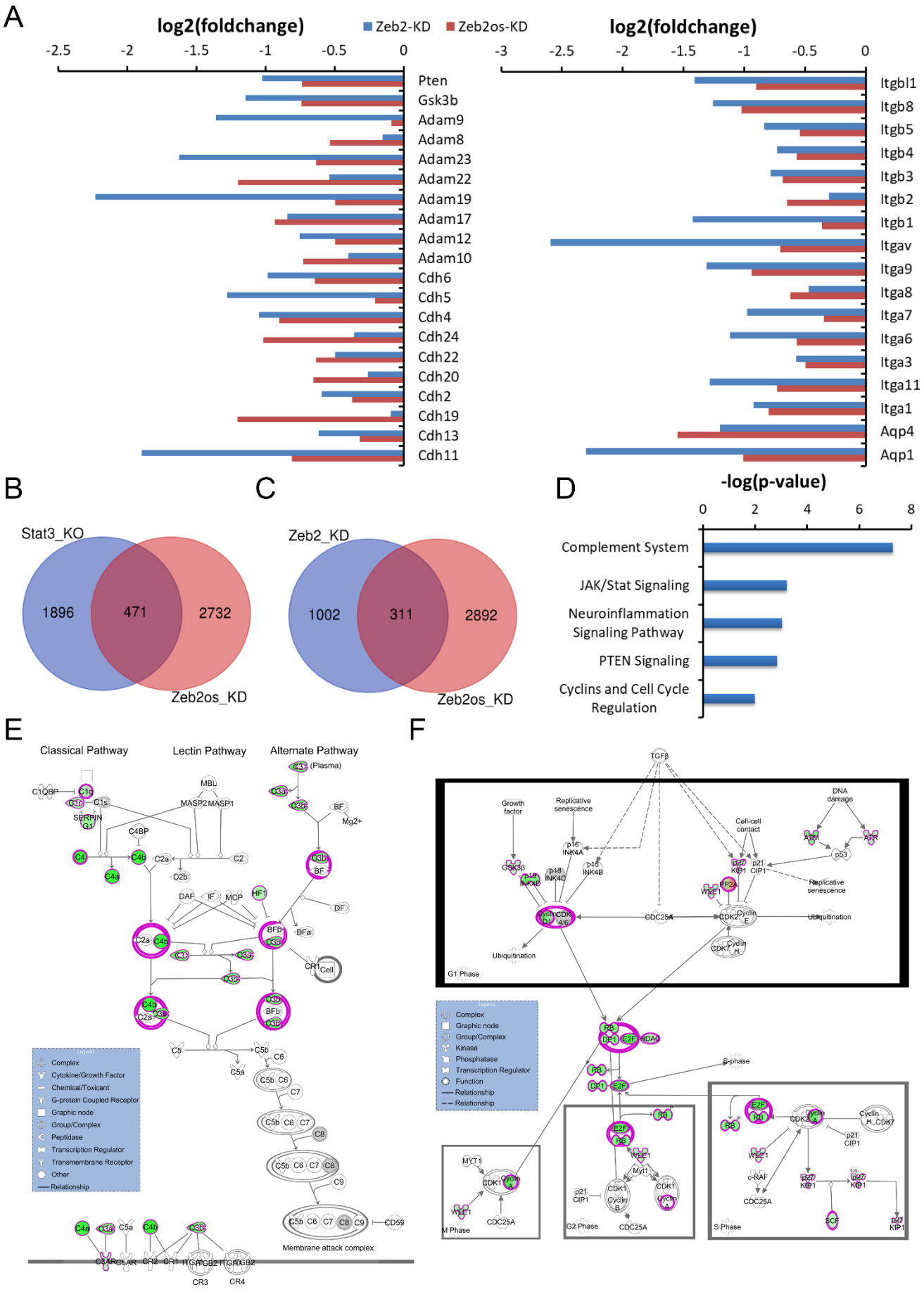
A
log2(foldchange)
Zeb2-KD
Zeb2os-KD
-2.5
-2
-1.5
-1
-0.5
0
Pten
Gsk3b
Adam9
Adam8
Adam23
Adam22
Adam19
Adam17
Adam12
Adam10
Cdh6
Cdh5
Cdh4
Cdh24
Cdh22
Cdh20
Cdh2
Cdh19
Cdh13
Cdh11
log2(foldchange)
-3
-2.5
-2
-1.5
-1
-0.5
0
Itgbl1
Itgb8
Itgb5
Itgb4
Itgb3
Itgb2
Itgb1
Itgav
Itga9
Itga8
Itga7
Itga6
Itga3
Itga11
Itga1
Aqp4
Aqp1
B
Stat3_KO
1896
471
2732
Zeb2os_KD
C
Zeb2_KD
1002
311
2892
Zeb2os_KD
D
-log(p-value)
0
2
4
6
8
Complement System
JAK/Stat Signaling
Neuroinflammation Signaling Pathway
PTEN Signaling
Cyclins and Cell Cycle Regulation
E
Classical Pathway
Lectin Pathway
Alternate Pathway
Membrane attack complex
F
TGFβ
G1 Phase
S-phase
G2 Phase
M Phase
S Phase

**Figure S6** Related to Figure 4. **(A)** The expression changes of in *Pten*, *Gsk3b*, as well as the families of Adam, Integrin, Aqp and Cdh genes in *Zeb2* KD vs. control and *Zeb2os* KD vs. control astrocytes. **(B)** Venn diagram showing the overlap of DEGs between *Stat3* KO and *Zeb2os* KD astrocytes. **(C)** Venn diagram showing the overlap of DEGs between *Zeb2* KD and *Zeb2os* KD astrocytes. **(D)** Ingenuity Pathway Analysis (IPA) shows significantly enriched canonical pathways for common DEGs between *Stat3* KO vs control and *Zeb2os* KD vs control astrocytes. **(E, F)** Genes in the complement system pathway **(E)** and cyclins and the cell cycle regulation pathway **(F)** are enriched in *Zeb2os* KD DEGs. FDR < 0.05. The intensity of green (decreased expression) indicates the degree of change in gene expression (log2|fold-change|).

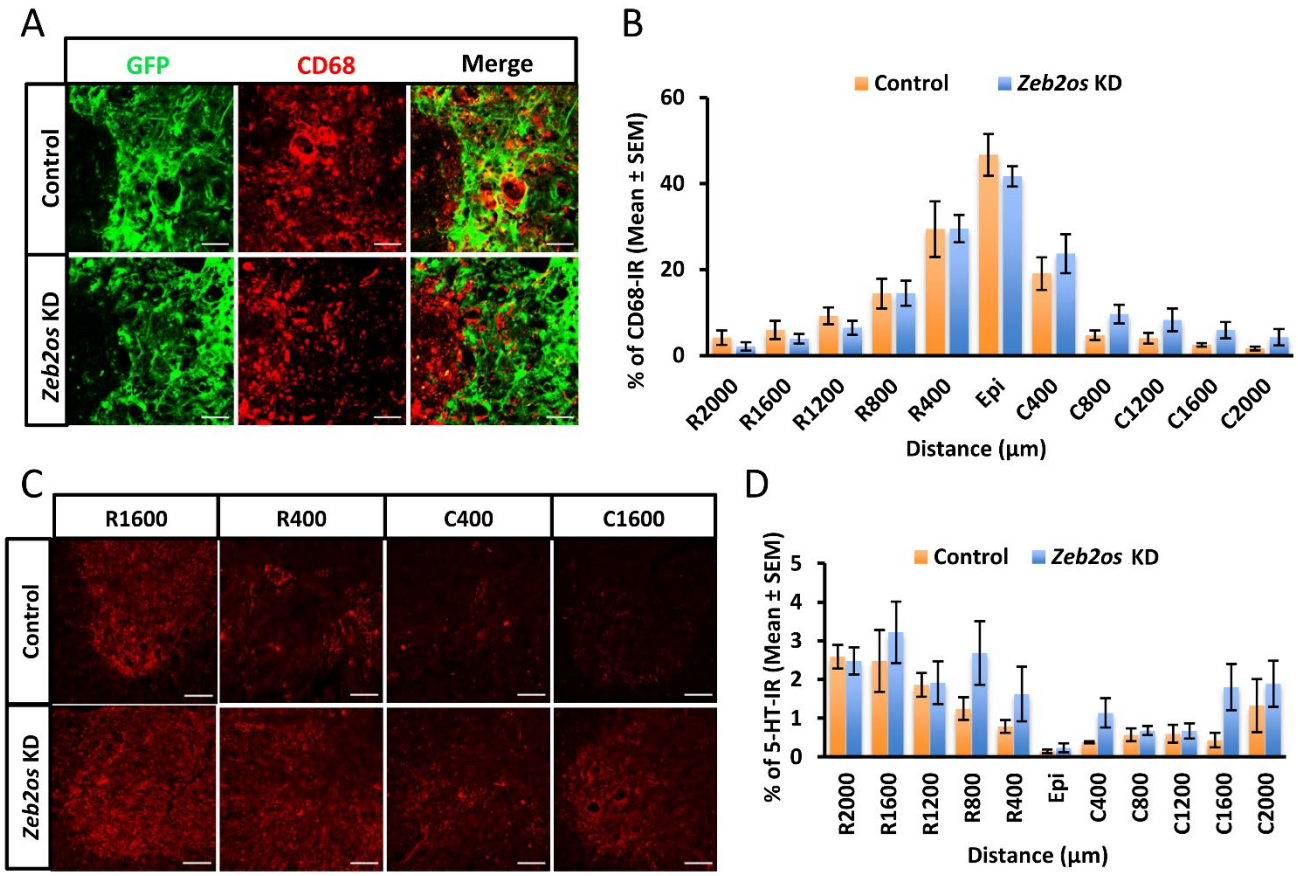


**Figure S7** Related to Figure 6. **(A)** Immunohistochemistry of CD68 (red) expression adjacent to AAV transduced astrocyte scar border (green) in *Zeb2os* KD compared with control at caudal 400 μm from the SCI epicenter (Scale bar = 40 μm). **(B)** Mean percentage of CD68-immunoreactive area in the total spinal cord sections at various distances from the SCI epicenter (Epi) ($n$ = 5-6). **(C)** Immunohistochemistry of 5-HT (white) expression at ventral horn in *Zeb2os* KD compared with control at 800, 2,000 μm rostral and 800, 1,600 μm caudal from the SCI epicenter (Scale bar = 60 μm). **(D)** Mean percentage of 5-HT-immunoreactive area in ventral horns at various distances from the SCI epicenter (Epi) ($n$ = 5). Data is presented as mean ±SEM; an independent $t$-test was performed to compared the difference between *Zeb2os* KD group with control group.